Search for Higgs Boson Produced in Association with a Vector Boson Using Like-Sign Dilepton Events in Run-II with 9.4 fb^{-1}

The CDF Collaboration
URL http://www-cdf.fnal.gov
(Dated: June 13, 2012)

We search for the neutral higgs production associated with a vector boson using high-p_T isolated like-sign dilepton events in $p\bar{p}$ collisions at $\sqrt{s} = 1.96$ TeV. The data were collected with the CDF-II detector at the Fermilab Tevatron collider and correspond to an integrated luminosity of 9.4 fb^{-1}. The expected number of background event is 696.1 $\pm$ 52.8 for the events with the first lepton p_T larger than 20 GeV/c and the second lepton p_T larger than 6 GeV/c , while we observe 624 events in the data to find no significant disagreements. The expected numbers of Wh and Zh events are 5.1 and 0.5, respectively, for the fermiophobic higgs of the mass 110 GeV/c^2 assuming the Standard Model production cross section. The expected numbers of events for the Standard Model higgs of the mass 160 GeV/c^2 are 1.5 and 0.2, respectively. We apply the Boosted Decision Tree technique for separating the backgrounds and signal events to improve the search sensitivity, then calculate limits in the Bayesian framework by using the output distributions. We obtain observed (expected) limits on the cross section ratio to be 4.4 $(2.6^{+1.1}_{-0.7})$ for the 110 GeV/c^2 fermiophobic higgs and 9.2 $(5.9^{+2.5}_{-1.6})$ for the 160 GeV/c^2 Standard Model higgs at the 95% confidence level.

I. INTRODUCTION

In the Standard Model, the higgs boson is introduced to explain the electroweak symmetry breaking and the origin of fermion masses [1]. The direct search at the CERN e^+e^- collider (LEP2) presents a lower limit on the higgs boson mass of $m_h > 114.4$ GeV/c^2 at the 95% confidence level (C.L.). Indirect measurements tells us that the mass of the Standard Model Higgs boson is lower than about 152 GeV/c^2 at the 95% C.L., and which increases to 171 GeV/c^2 when the direct search is included [2].

Our physics objective is to search for the low-mass fermiophobic higgs and the high-mass Standard Model higgs boson using like-sign dilepton events produced by

$$qq' \to Vh \to VW^*W^* \to \ell^\pm \ell^\pm + X, \quad V = W, Z.$$

The brancing fractions for the fermiophobic higgs are higher than the Standard Model higgs boson, especially in the low-mass region. The relevant regions of the higgs mass are above 110 GeV/c^2 for the fermiophobic higgs where the branching fraction of $h \to W^*W^*$ supersedes that of $h \to \gamma\gamma$, and above 135 GeV/c^2 for the Standard Model higgs where the branching fraction of $h \to b\bar{b}$ is overtaken by this channel.

The fermiophobic higgs boson has no coupling to the fermions [3]. Existence of the fermiophobic higgs could be an indication that the origin of particle masses would be different for the bosons and the fermions. Such a particle can also arise as a CP-even scalar h^0 in the two higgs doublet model (2HDM) type I. The model has seven degrees of freedom: the five particle masses ($h^0, H^0, A^0, H^\pm$) and two angles (α, β). In the type I, the lightest CP-even scalar h^0 couples to a fermion proportionally to $\cos\alpha$, and the h^0 becomes a fermiophobic higgs when $\alpha = \pi/2$.

II. DATA SAMPLE & EVENT SELECTION

This analysis is based on the data with an integrated luminosity of 9.4 fb^{-1} collected with the CDF-II detector between March 2002 and Sep 2011. Detailed descriptions of the CDF-II detector can be found in [4]. The data are collected with inclusive lepton triggers that requires an electron with transverse energy (E_T) > 18 GeV or a muon with transverse momentum (p_T) > 18 GeV/c. Starting from the inclusive lepton datasets, we apply a number of event selection criteria to obtain a baseline dilepton sample. The events are required to have primary vertices within the region to ensure well-defined measurement of collisions by the detector and to pass a cosmic-ray veto. We select events at least one electron with $E_T > 20$ GeV and $p_T > 10$ GeV/c, or muon with $p_T > 20$ GeV/c, which is considered to be responsible for firing the triggers we have chosen, and at least one other electron with $E_T > 6$ GeV and $p_T > 6$ GeV/c, or muon with $p_T > 6$ GeV/c, as the baseline dilepton selection. The leptons must be found in the central detector ($|\eta| < 1.1$) for electrons and muons, or forward region ($1.2 < |\eta| < 1.7$) for muons within fiducial regions of the sub-detectors. They are also required to be isolated in terms of the calorimeter cone-isolation, with a cone size of $R = 0.4$, to be less than 2 GeV, where $R = \sqrt{(\Delta\eta)^2 + (\Delta\phi)^2}$ is the radius in the η-ϕ space, $\eta = -\ln(\tan\theta/2)$ is the pseudorapidity, the θ is the polar angle with respect to the proton beam direction, and ϕ is the azimuthal angle. The leptons must have a well-measured track, found both in the outer tracking chamber and the inner silicon detector, with the z coordinate and the impact parameter at the closest approach point to the beamline being consistent with coming from the primary vertex. We then apply a cut for lepton identification based on the likelihood method, which collects several probability density functions in each signal and background. The method is originally introduced in low-p_T electron tagging [5]. We choose the signal as the lepton in high-p_T lepton samples, and the background as the fake lepton in the jet samples. If the electron is consistent with being due to a photon conversion as indicated by the presence of an additional nearby track, the electron is vetoed.

For the exactly two-lepton events passing our selection above, we explicitly require a cut to ensure that the two leptons are coming from the same vertex, and also apply a dilepton mass cut ($M_{\ell\ell} > 12$ GeV/c^2) and a Z-event veto. Finally, we require the like-sign charge combination.

III. ACCEPTANCE AND EXPECTED EVENTS FOR SIGNAL

We estimate the number of expected events for Wh and Zh for higgs mass of 110-200 GeV/c^2 passing event selections. The branching fraction corresponding to events with at least 2 leptons from VWW is about 0.12. The expected number of events are 0.7-5.6 for fermiophobic higgs, and 0.3-1.8 events for SM higgs. TABLE I shows the theoretical cross section and branching fraction ($h \to WW$) in each higgs mass to be used in the estimation of expected events. TABLE II shows the expected events for signal events in each higgs mass, the uncertainties include MC statistics and systematic uncertainties.

IV. BACKGROUNDS

Although the like-sign requirement is quite effective to suppress QCD and known electroweak processes, we expect that fake-lepton backgrounds and residual photon-conversions still remain at a considerable level in the events of our signature. They are estimated by data-driven methods, while other backgrounds containing prompt real-leptons (physics backgrounds) are estimated by Monte Carlo (MC) samples.

A. Physics Backgrounds

The physics backgrounds can be classified into reducible and irreducible backgrounds. The reducible backgrounds are Drell-Yan, WW, $t\bar{t}$, and W + (heavy-flavor hadrons), while irreducible backgrounds are WZ and ZZ. The reducible backgrounds are reduced by the isolation cut and like-sign requirement. Since fake-leptons and residual photon-conversions are estimated separately using real data, we reject them found in the MC by looking at the generator-level information to avoid double counting. For irreducible backgrounds, those contributions are small due to their small production cross sections.

B. Residual Photon-Conversion Background

The residual photon-conversion backgrounds arise from an electron originating from the photon conversion with an unobserved partner track due to its low momentum. We estimate the backgrounds by multiplying lepton + conversion events by residual photon-conversion rate (R_{res}). We define the rate by

$$R_{\mathrm{res}} = \frac{1 - \varepsilon_{\mathrm{con}}}{\varepsilon_{\mathrm{con}}},$$

where $\varepsilon_{\mathrm{con}}$ is the conversion detection efficiency. The efficiency is measured by comparing the conversions found in the real data with conversion MC samples that are tuned to match with the sub-sample of real conversions in the high-p_T region of partner-tracks where the efficiency is well known. The residual conversion rate is parametrized by the parent photon p_T.

C. Fake Lepton Background

The fake electron backgrounds are interactive $\pi^{\pm}$, overlap of π^0 and a track, and residual photon-conversions. The fake muon backgrounds are punch-through hadrons and decay-in-flight muons from $\pi^{\pm}$ and $K^{\pm}$. We also regard leptons from semileptonic decays of heavy-flavor hadron as one of fake lepton backgrounds. These background objects are common in generic QCD events. We estimate the backgrounds by multiplying lepton + isolated track events by the fake lepton rates derived from inclusive jet samples. The fake lepton rate (R_{fake}) is defined as a rate of leptons in the jet samples relative to isolated tracks with certain energy depositions especially in the hadron calorimeters. The p_T cut is 6 GeV/c in accordance with the lower p_T cut of our event selection. We reject W and Z events in the jet samples to avoid prompt real-leptons from electroweak processes by using MC-based subtractions. And the fake rates are parametrized by six variables: p_T , isolation, pseudorapidity η, impact parameter d_0, ϕ within the wedge in the calorimeter, $\Delta\phi$ between lepton and missing E_T. The fake electon rate are corrected by subracting residual conversions in the jet samples because we estimate the amount of residual photon-conversion events separately as mentioned in the previous section.

D. Expected Backgrounds

We look at the consistency between the data and background expectations in these regions:

- Side-Band: 2nd lepton failing the lepton identification and passing other selections (to confirm our fake lepton estimation),

- Zero-Silicon: 2nd lepton with no silicon hits and passing other selections (The 2nd lepton coming from conversion events mainly, so the region is used to validate the estimation of the residual conversion events),

- Opposite-Sign: charge combination is opposite-sign and all selections are required (to check the scale factors between data and Monte Carlo samples),

- Like-Sign: charge combination is like-sign and this is the signal region,

where we require all selection of the first lepton. The numbers are shown in TABLE III, and we see no significant discrepancies between them.

V.   BOOSTED DECISION TREE

We employ a multivariate analysis based on the Boosted Decision Tree (BDT) technique [6] to get more search sensitivity. We train the BDT using fake leptons and residual photon-conversions, because they are dominant backgrounds for our LS dilepton analysis. We perform the training in each mass of the higgs sample independently, using nine variables as the BDT inputs:

- 1st lepton p_T (p_{T1}),

- 2nd lepton p_T (p_{T2}),

- Dilepton system p_T (p_{T12}),

- Missing E_T,

- Dilepton mass,

- MetSpec : $\not{E}_T$ if $\Delta\phi(\not{E}_T, \ell$ or jet$) > \pi/2$ or
       : $\not{E}_T \sin(\Delta\phi(\not{E}_T, \ell$ or jet$))$ if $\Delta\phi(\not{E}_T, \ell$ or jet$) < \pi/2$,

- H$_T$ (Sum of p_{T1}, p_{T2}, jets E_T ($E_T > 15$ GeV and $|\eta| < 2.0$), and Missing E_T)

- Number of Jets with $E_T > 15.0$ GeV,

- Sphericity,

- Aplanarity.

FIG 1 and 2 show the BDT input variables for LS dilepton events. FIG 3 shows the BDT outputs for LS dilepton events from the BDT trained for the $m_H = 110$ and 160 GeV/c^2.

VI.   SYSTEMATIC UNCERTAINTY

The systematic uncertainties are estimated for the normalization (rate) systematic and the shape of the BDT outputs. TABLE IV, V, and VI are summaries of the rate systematic uncertainties for Wh, Zh and backgrounds. In those tables, Z/γ^* comes from the discrepancy between data and expected events, which is used for the scale factor validation between data and Monte Calro samples. Also, we estimate the shape systematic uncertainties which come from jet energy scale by shifting $\pm 1\sigma$ from the default correction factor[7], and include when calculate the 95% C.L. upper limits in the next section.

VII.   RESULTS

We see no significant discrepancies between background expectations and the data in the BDT outputs. Using these output distributions, we set the ratios of the 95% C.L. upper limits on the cross section times branching fraction $\sigma(p\bar{p} \to Vh) \times Br(h \to WW)$ to the prediction for fermiophobic higgs (assuming the Standard Model production cross sections) and for the Standard Model, which are shown in TABLE VII and VIII, respectively. Also those plots are shown in FIG. 4 and 5.

VIII.   CONCLUSIONS

We searched for the neutral higgs production associated with the vector boson using high-p_T like-sign dilepton events using the data corresponding to an integrated luminosity of 9.4 fb^{-1}. The expected number of backgrounds in the final sample was 696.1 $\pm$ 52.8, while the actual number of observed events was 624. The expected number of signal events was 5.6 for the fermiophobic higgs of the mass 110 GeV/c^2 assuming the Standard Model production cross section and 1.7 for the Standard Model higgs of 160 GeV/c^2. We employed the Boosted Decision Tree technique for separating backgrounds and signal events in the final sample, and found no significant disagreements in the output distributions. We obtained the upper limits on the production cross-section times the branching fraction for the higgs with masses in the region from 110 GeV/c^2 to 200 GeV/c^2. The expected limit on the ratio to the theoretical prediction for the cross section was 2.6 for the fermiophobic higgs of the mass 110 GeV/c^2 and 5.9 for the Standard Model higgs of the mass 160 GeV/c^2, while the observed limits were 4.4 and 9.2, respectively.

TABLE I: Theoretical cross sections and branching fractions in each higgs mass.

$Vh{\to}VW^*W^*{\to}l^{\pm}l^{\pm}+X$			CDF Run-II Preliminary: 9.4 fb^{-1}	
Higgs Mass (GeV/c^2)	$\sigma(p\bar{p}{\to}Wh)$ (fb)	$\sigma(p\bar{p}{\to}Zh)$ (fb)	$B_F(h{\to}WW)$ (Fermiophobic higgs)	$B_F(h{\to}WW)$ (SM higgs)
110	203.7	120.2	0.85	0.05
120	150.1	90.2	0.87	0.14
130	112.0	68.5	0.87	0.30
140	84.6	52.7	0.87	0.50
150	64.4	40.8	0.89	0.70
160	48.5	31.4	0.95	0.91
170	38.5	25.3	0.97	0.96
180	30.1	20.0	0.94	0.93
190	24.0	16.1	0.79	0.79
200	19.1	13.0	0.74	0.74

TABLE II: Expected number of events for signal passing baseline event selections (FP: Fermiophobic Higgs).

$Vh{\to}VW^*W^*{\to}l^{\pm}l^{\pm}+X$					CDF Run-II Preliminary: 9.4 fb^{-1}	
Higgs Mass	Wh Expected Events	Wh Expected Events	Zh Expected Events	Zh Expected Events	Total	Total
(GeV/c^2)	(FP)	(SM)	(FP)	(SM)	(FP)	(SM)
110	5.1±0.6	0.29±0.03	0.53±0.06	0.030±0.004	5.6±0.6	0.32±0.03
120	4.0±0.5	0.66±0.08	0.43±0.05	0.07±0.01	4.4±0.7	0.73±0.08
130	3.2±0.4	1.1±0.1	0.36±0.04	0.13±0.01	3.6±0.4	1.2±0.1
140	2.6±0.3	1.5±0.2	0.30±0.03	0.17±0.02	2.9±0.3	1.7±0.2
150	2.1±0.2	1.6±0.2	0.24±0.03	0.19±0.02	2.3±0.2	1.8±0.2
160	1.6±0.2	1.5±0.2	0.18±0.02	0.18±0.02	1.8±0.2	1.7±0.1
170	1.3±0.1	1.3±0.1	0.15±0.02	0.15±0.02	1.5±0.1	1.5±0.1
180	1.0±0.1	1.0±0.1	0.12±0.01	0.12±0.01	1.1±0.1	1.1±0.1
190	0.75±0.08	0.75±0.08	0.09±0.01	0.09±0.01	0.84±0.08	0.84±0.08
200	0.59±0.07	0.59±0.07	0.07±0.01	0.07±0.01	0.66±0.07	0.66±0.07

TABLE III: Background expectation and observed number of events for side-band, zero-silicon, opposite-sign and like-sign(signal) dilepton events.

$Vh \to VW^*W^* \to l^\pm l^\pm + X$			CDF Run-II Preliminary: 9.4 fb^{-1}	
	Lepton ID Side-Band	Zero Silicon	OS	Signal
Fakes	4493.9±594.6	15.7±2.53	674.8±107.6	631.9±51.4
Photon-conversions	123.1±34.1	91.7±13.0	192.5±39.6	49.5±12.1
Total	4616.9±595.6	107.4±13.2	867.3±114.7	681.4±52.8
$Z/\gamma^* \to ee$	-	-	19841.4±1503.9	-
$Z/\gamma^* \to \mu\mu$	-	-	30327.3±2296.2	-
$Z/\gamma^* \to \tau\tau$	-	-	4071.3±310.2	-
$t\bar{t}$	-	-	269.2±20.4	-
WW	-	-	399.2±30.2	-
WZ	2.1±0.3	-	27.3±3.4	13.1±1.6
ZZ	0.4±0.1	-	23.7±3.0	1.7±0.2
Total MC	2.5±0.3	-	54959.4±4159.2	14.8±1.7
Fermiophobic higgs (Wh110)	0.88±0.10	-	6.31±0.71	5.09±0.59
Fermiophobic higgs (Zh110)	0.10±0.01	-	2.33±0.27	0.53±0.06
Fermiophobic Total (110)	0.98±0.10	-	8.64±0.76	5.62±0.59
SM higgs (Wh160)	0.19 ±0.02	-	2.46±0.28	1.51±0.17
SM higgs (Zh160)	0.028±0.003	-	1.15±0.13	0.18±0.02
SM Total (160)	0.21±0.02	-	3.61±0.31	1.69±0.17
Total expected	4619.4±595.6	107.4±13.2	55826.7±4214.6	696.1±52.8
Data	4598	127	51243	624

TABLE IV: Rate systematic uncertainty for the Wh Events.

$Wh \to WW^*W^* \to l^\pm l^\pm + X$					CDF Run-II Preliminary: 9.4 fb^{-1}					
Higgs Mass (GeV/c^2)	110	120	130	140	150	160	170	180	190	200
Statistics	0.8%	0.8%	0.8%	0.7%	0.7%	0.7%	0.7%	0.7%	0.7%	0.7%
PDF	2.2%	1.9%	1.6%	1.6%	1.4%	1.2%	1.4%	1.1%	0.8%	0.7%
ISR	4.0%	4.0%	4.0%	4.0%	4.0%	4.0%	4.0%	4.0%	4.0%	4.0%
FSR	5.3%	5.3%	5.3%	5.3%	5.3%	5.3%	5.3%	5.3%	5.3%	5.3%
Z/γ^*	4.6%	4.6%	4.6%	4.6%	4.6%	4.6%	4.6%	4.6%	4.6%	4.6%
Cross Section	5.0%	5.0%	5.0%	5.0%	5.0%	5.0%	5.0%	5.0%	5.0%	5.0%
Luminosity	6.0%	6.0%	6.0%	6.0%	6.0%	6.0%	6.0%	6.0%	6.0%	6.0%
Total	11.5%	11.4%	11.4%	11.4%	11.3%	11.3%	11.3%	11.3%	11.3%	11.3%

TABLE V: Rate systematic uncertainty for the Zh Events.

$Zh \to ZW^*W^* \to l^\pm l^\pm + X$					CDF Run-II Preliminary: 9.4 fb^{-1}					
Higgs Mass (GeV/c^2)	110	120	130	140	150	160	170	180	190	200
Statistics	2.3%	2.2%	2.1%	2.1%	2.0%	2.1%	2.1%	2.1%	1.9%	1.9%
PDF	2.5%	2.0%	1.5%	1.8%	1.8%	1.3%	1.3%	1.0%	1.1%	0.4%
ISR	4.0%	4.0%	4.0%	4.0%	4.0%	4.0%	4.0%	4.0%	4.0%	4.0%
FSR	5.3%	5.3%	5.3%	5.3%	5.3%	5.3%	5.3%	5.3%	5.3%	5.3%
Z/γ^*	4.6%	4.6%	4.6%	4.6%	4.6%	4.6%	4.6%	4.6%	4.6%	4.6%
Cross Section	5.0%	5.0%	5.0%	5.0%	5.0%	5.0%	5.0%	5.0%	5.0%	5.0%
Luminosity	6.0%	6.0%	6.0%	6.0%	6.0%	6.0%	6.0%	6.0%	6.0%	6.0%
Total	11.7%	11.6%	11.5%	11.6%	11.6%	11.5%	11.5%	11.5%	11.4%	11.4%

TABLE VI: Rate systematic uncertainty for backgrounds.

$Vh{\rightarrow}VW^*W^*{\rightarrow}l^\pm l^\pm + X$		CDF Run-II Preliminary: 9.4 fb^{-1}		
	Fake leptons	Residual photon-conversion	WZ	ZZ
Statistics	2.1%	11.1%	0.7%	2.1%
Fake rate	7.9%	-	-	-
Residual conversion rate	-	22.0%	-	-
Z/γ^*	-	-	4.6%	4.6%
Cross Section	-	-	10.0%	10.0%
Luminosity	-	-	6.0%	6.0%
Total	8.2%	24.7%	12.6%	12.7%

TABLE VII: Upper limits on the production cross-section times branching fraction $\sigma(p\bar{p}{\rightarrow}Vh) \times B_F(h{\rightarrow}W^{*+}W^{*-})$ relative to the prediction for fermiophobic higgs.

$Vh{\rightarrow}VW^*W^*{\rightarrow}l^\pm l^\pm + X$					CDF Run-II Preliminary: 9.4 fb^{-1}
Mass (GeV/c^2)		(Expected limit)/FP			(Observed limit)/FP
	-2σ	-1σ	Median	$+1\sigma$ $+2\sigma$	
110	1.4	1.9	2.6	3.7 5.0	4.4
120	1.6	2.2	3.0	4.3 6.0	5.3
130	1.9	2.5	3.5	4.9 7.0	5.8
140	2.2	2.9	4.0	5.6 7.8	6.6
150	2.6	3.4	4.7	6.7 9.3	6.6
160	3.1	4.1	5.6	8.0 11.1	8.8
170	3.6	4.7	6.4	9.1 12.8	10.3
180	4.4	5.7	7.8	11.1 15.5	11.3
190	6.0	7.7	10.6	15.0 20.7	16.3
200	7.5	9.7	13.3	18.9 26.5	20.1

TABLE VIII: Upper limits on the production cross-section times branching fraction $\sigma(p\bar{p}{\rightarrow}Vh) \times B_F(h{\rightarrow}W^{*+}W^{*-})$ relative to the prediction for the Standard Model higgs.

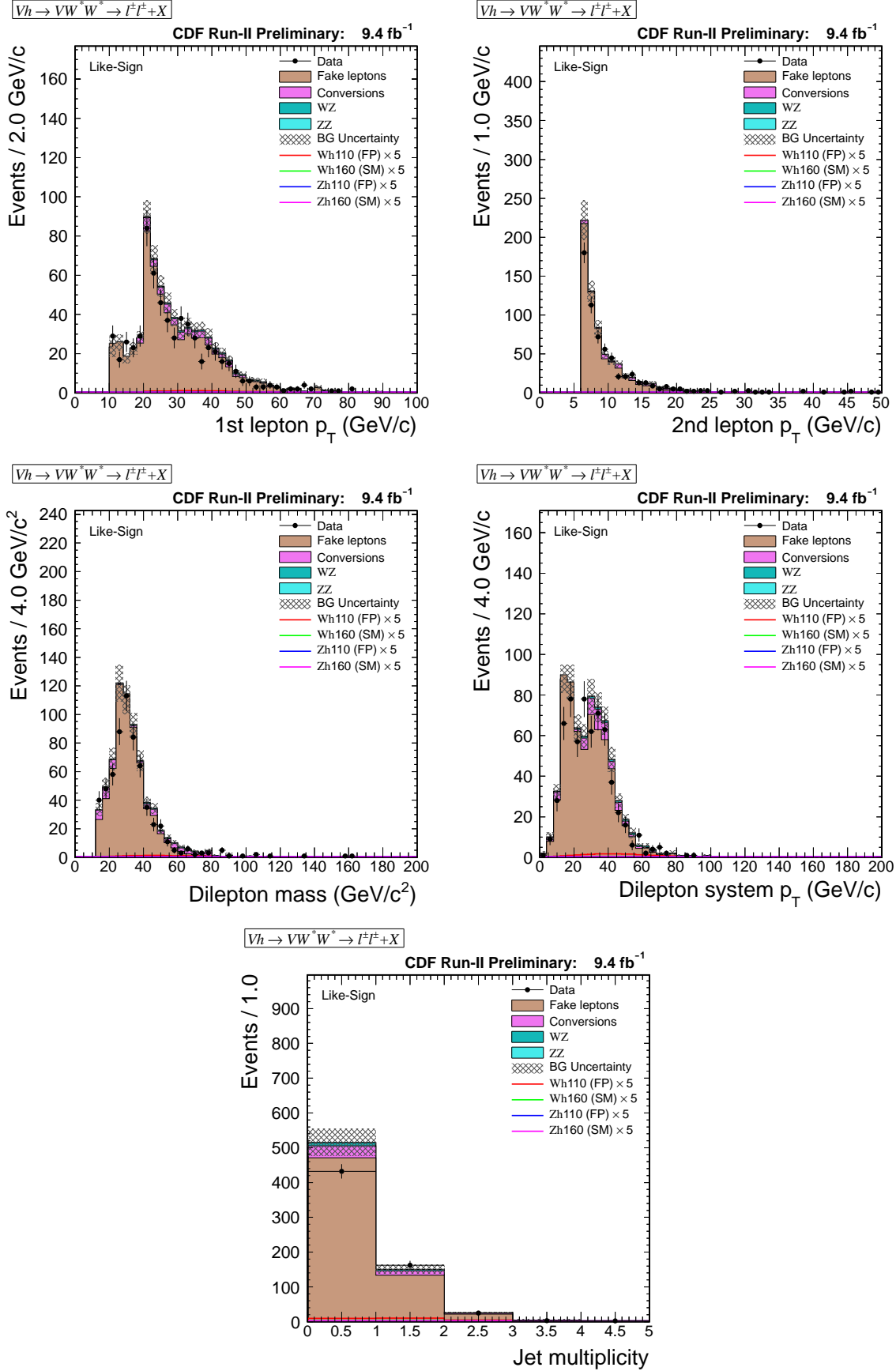| $Vh{\rightarrow}VW^*W^*{\rightarrow}l^\pm l^\pm + X$					CDF Run-II Preliminary: 9.4 fb^{-1}
Mass (GeV/c^2)		(Expected limit)/SM			(Observed limit)/SM
	-2σ	-1σ	Median	$+1\sigma$ $+2\sigma$	
110	24.9	32.8	45.8	65.1 89.0	77.2
120	10.0	13.2	18.3	26.1 36.2	32.5
130	5.5	7.2	10.0	14.1 19.9	16.4
140	3.8	5.0	6.9	9.7 13.4	11.4
150	3.3	4.3	6.0	8.5 11.8	8.3
160	3.3	4.3	5.9	8.4 11.6	9.2
170	3.7	4.7	6.5	9.2 12.9	10.4
180	4.5	5.7	7.9	11.2 15.6	11.4
190	6.0	7.7	10.6	15.0 20.8	16.4
200	7.6	9.7	13.3	18.9 26.5	20.2

FIG. 1: BDT input variables (1st lepton $p_T (p_{T1})$, 2nd lepton $p_T (p_{T2})$, Dilepton mass, Dilepton system $p_T (p_{T12})$, and Number of jets).
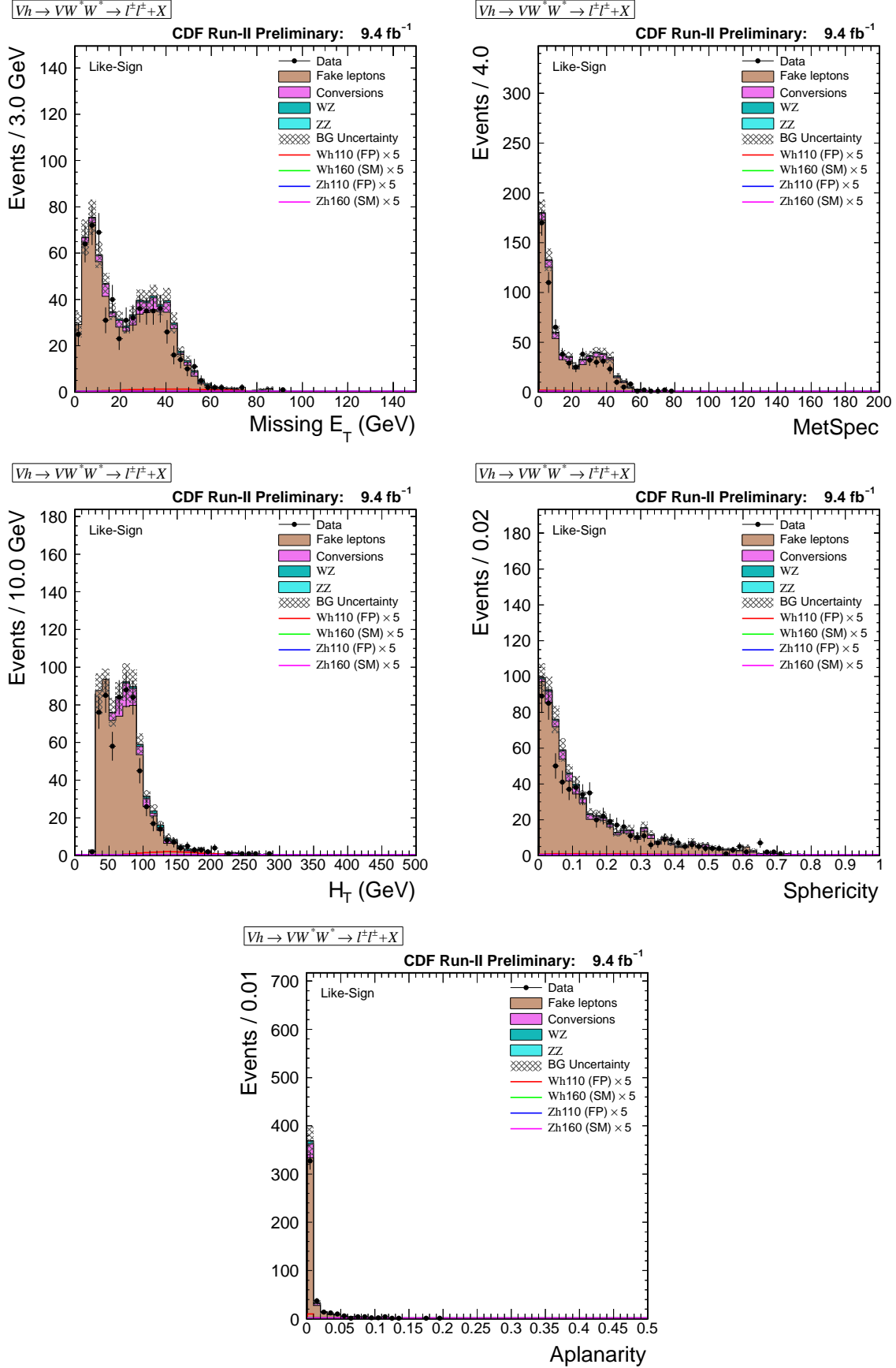
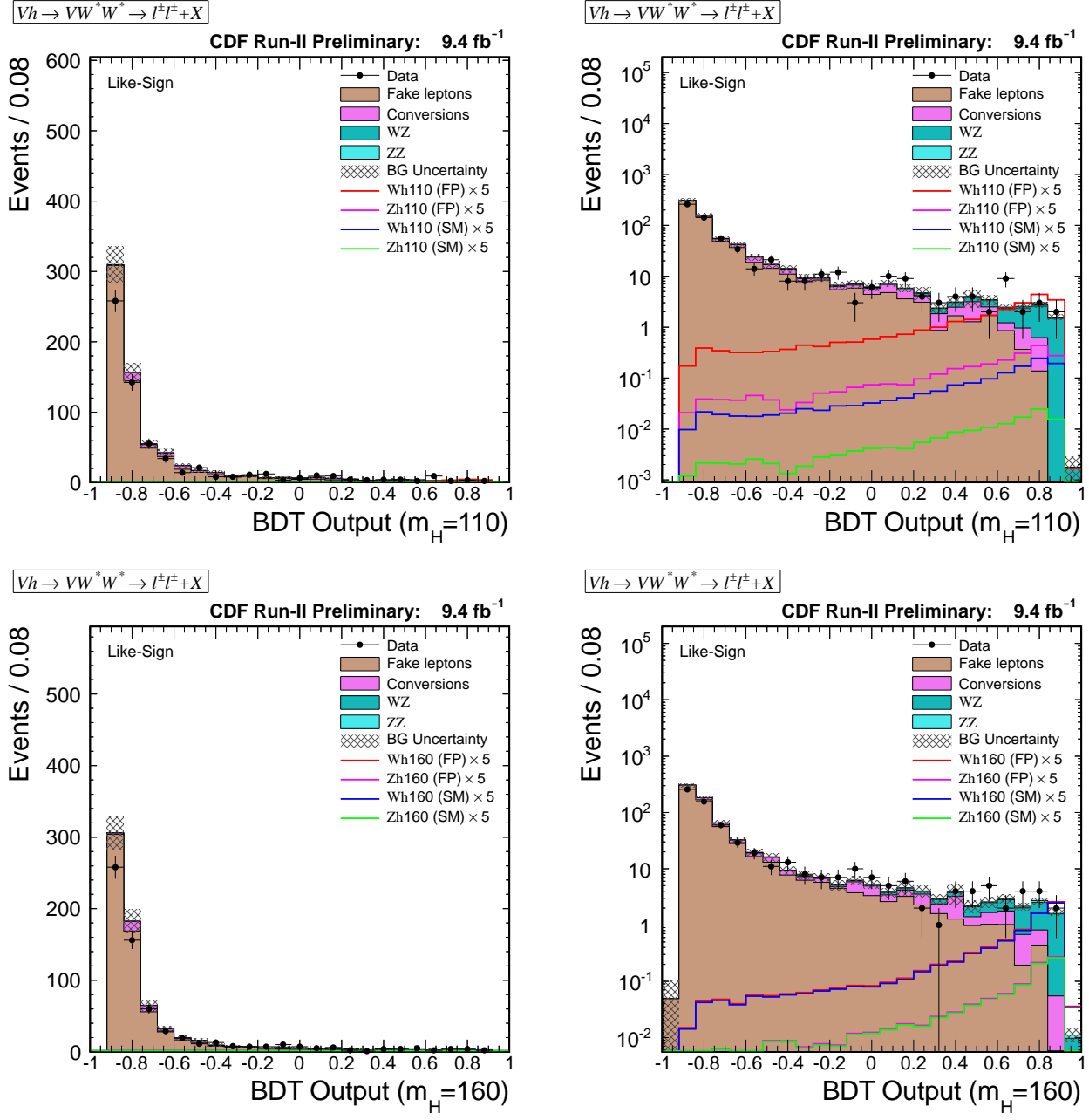FIG. 2: BDT input variables (Missing E_T, MetSpec, H_T, Sphericity, and Aplanarity).
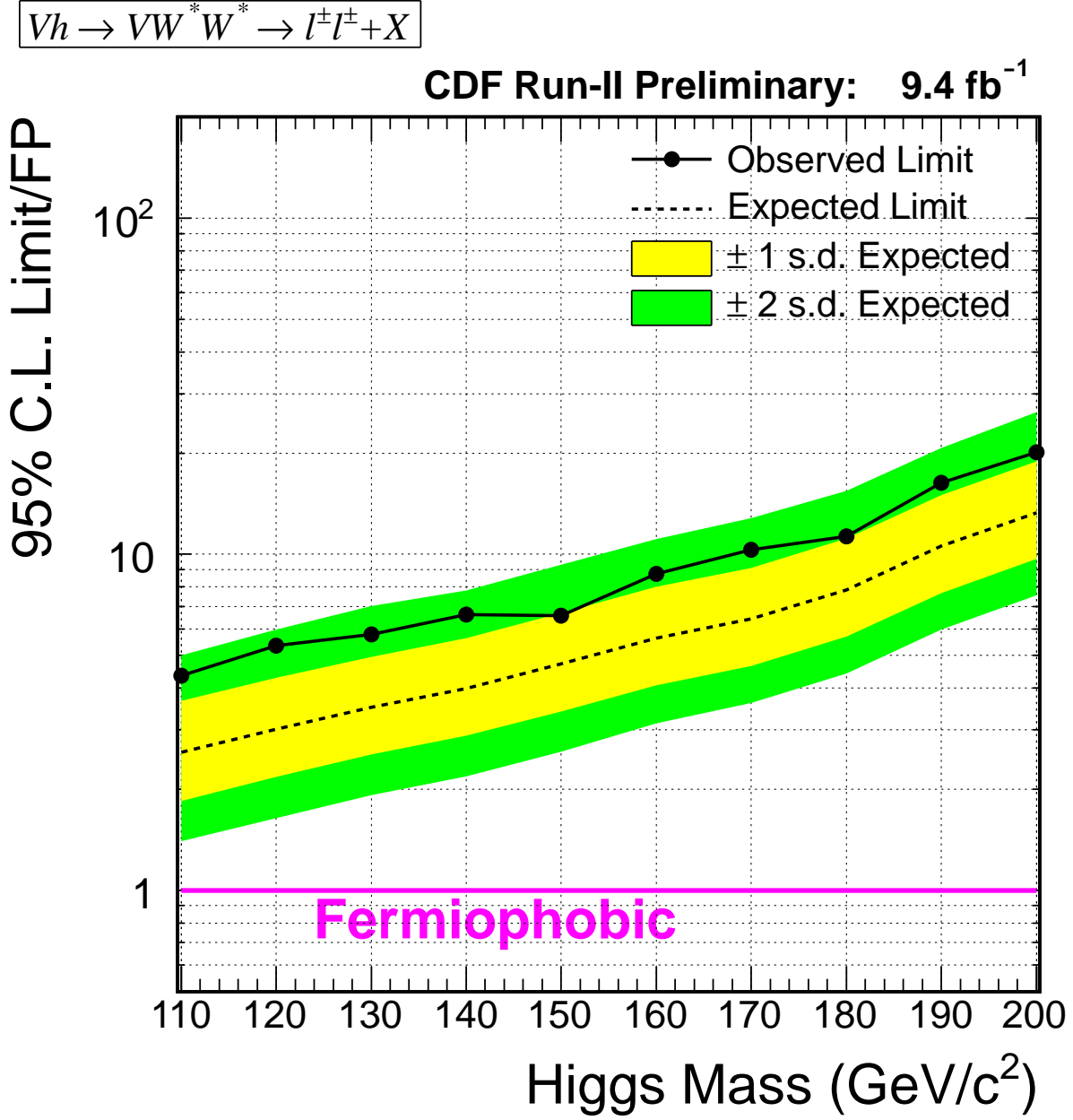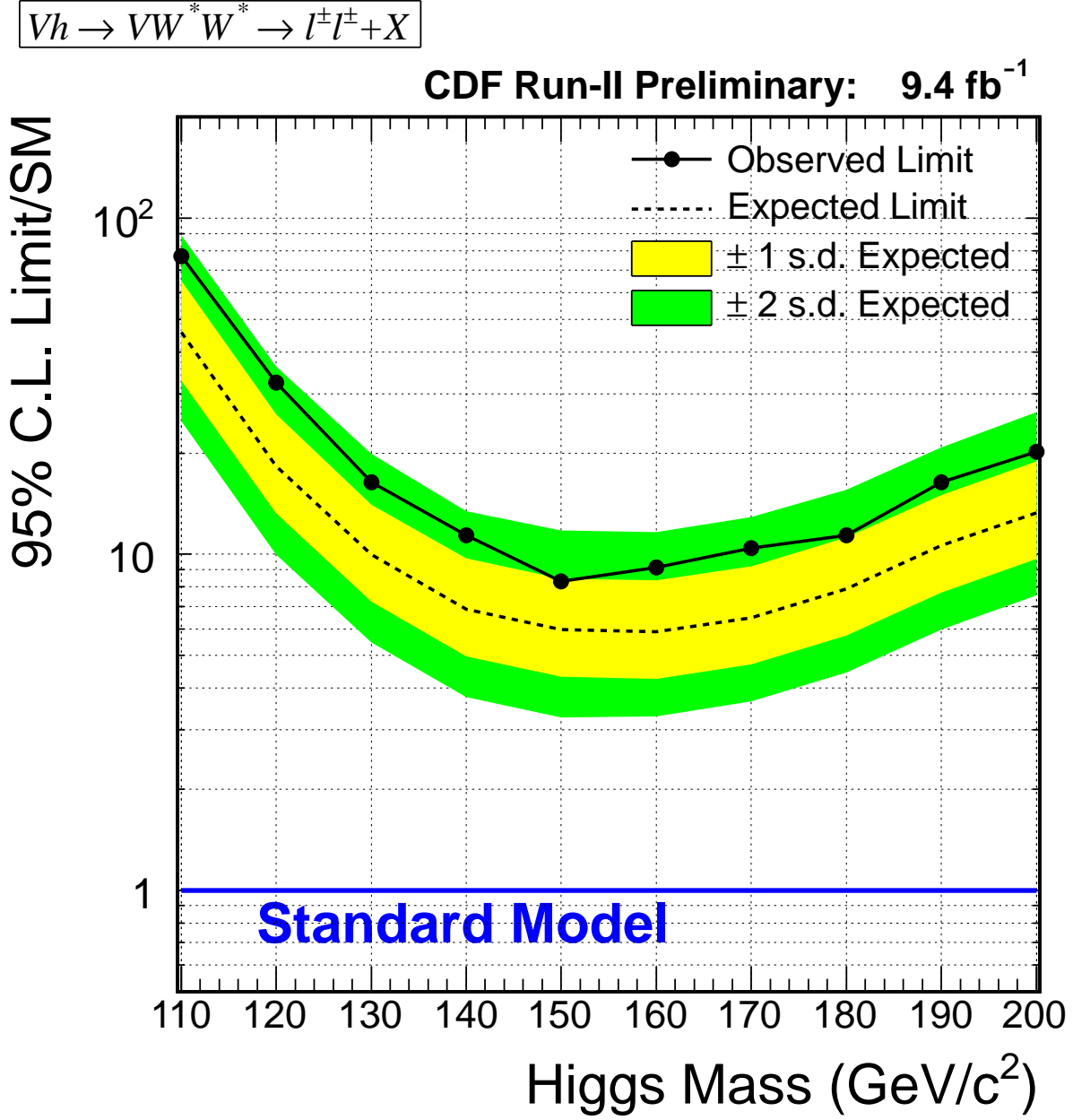
FIG. 3: BDT outputs for $m_H = 110$ and 160 GeV/c^2.

FIG. 4: Upper limits on the production cross-section times branching fraction $\sigma(p\bar{p}{\to}Vh) \times B_F(h{\to}W^{*+}W^{*-})$ relative to prediction for fermiophobic higgs at a 95% C.L. as a function of higgs mass.

FIG. 5: Upper limits on the production cross-section times branching fraction $\sigma(p\bar{p}{\rightarrow}Vh) \times B_F(h{\rightarrow}W^{*+}W^{*-})$ relative to prediction for SM higgs at a 95% C.L. as a function of higgs mass.

Acknowledgments

[1] P. W. Higgs, Phys. Rev. **145** 1156-1163(1966); P. W. Higgs, Phys. Rev. Lett. **13** 508-509 (1964).

[2] LEP Electroweak Working Group, http://lepwwg.web.cern.ch/LEPEWWG/.

[3] A. Stange, W. Maricano, and S. Willenbrock, Phys. Rev. D **49**, 1354 (1994).

[4] F. Abe, et al., Nucl. Instrum. Methods Phys. Res. A **271**, 387 (1988); D. Amidei, et al., Nucl. Instum. Methods Phys. Res. A **350**, 73 (1994); F. Abe, et al., Phys. Rev. D **52**, 4784 (1995); P. Azzi, et al., Nucl. Instrum. Methods Phys. Res. A **360**, 137 (1995); The CDFII Detector Technical Design Report, Fermilab-Pub-96/390-E

[5] V. Tiwari, G. Giurgiu, M. Paulini, J. Russ and B. Wicklund, "Likelihood Based Electron Tagging", CDF Public Note 7121.

[6] A. Hocker, P. Speckmayer, J. Stelzer, F. Tegenfeldt, H. Voss, K. Voss, "TMVA Toolkit for Multivariate Data Analysis with ROOT Users Guide".

[7] A. Bhatti et al., Nucl. Instrum. Methods, A **566**, 375 (2006).